Clays and Clay Minerals, Vol. 39, No. 1, 1–13, 1991.

TRANSMISSION ELECTRON MICROSCOPIC STUDY OF THE KAOLINITIZATION OF MUSCOVITE[1]

WEI-TEH JIANG AND DONALD R. PEACOR

Department of Geological Sciences, The University of Michigan
Ann Arbor, Michigan 48109

Abstract—Hydrothermally kaolinitized muscovite from the Otago schist of Brighton, New Zealand, has been studied by transmission and analytical electron microscopy (TEM and AEM) to determine the mechanism of alteration and to compare reactant-product relations for di- and trioctahedral micas. The muscovite is a primary metamorphic phase having a phengitic composition. It occurs as well-ordered, two- and three-layer polytypes, in grains as thick as 30 μm. Kaolinite occurs as packets of layers, each about 100–600 Å thick, which alternate with packets of muscovite or smectite-like layers. Most of the kaolinite is highly disordered in stacking sequence, although a one-layer polytype is also present, occurring as relatively thick sequences of layers. Phase boundaries between kaolinite and muscovite are invariably parallel to the 001 lattice fringes with no strain contrast; i.e., no transitions exist along layers. Parallelism of 00*l* and 11*l* reflection rows of both kaolinite and muscovite implies a topotaxial intergrowth. A smectite-like phase is also present, occurring as packets of wavy layers, which locally have periodic contrast that may reflect R1 ordering of illite/smectite. This material appears to be a direct, "along-layer" alteration product of muscovite. Electron diffraction data and lattice-fringe images imply that kaolinite alternates with micaceous phase(s) with some regularity; i.e., micaceous layers are separated by approximately equal numbers of kaolinite layers. Similar long-range periodicity occurs in contrast variations within packets of kaolinite layers.

The data collectively suggest that the alteration interface was self-perpetuating and that alteration proceeded rapidly along layers once it initiated in 2:1 layers at crystal edges or strained areas, with no observable component normal to the layers. They also suggest that smectite may have formed as an intermediate phase during the hydrothermal kaolinitization of muscovite. In the previous study of alteration of biotite in the same sample, "along-layer" transition boundaries were commonly observed, and a second, intermediate product phase was not detected, implying a relation between the alteration mechanisms and the chemical differences between reactants and products.

Key Words—Analytical electron microscopy, Hydrothermal alteration, Kaolinite, Muscovite, Transmission electron microscopy.

INTRODUCTION

Kaolinite is common in hydrothermally altered rocks (e.g., Nagasawa, 1978; Craw *et al.*, 1982; Beaufort and Meunier, 1983; Dudoignon *et al.*, 1988; Murray, 1988). Processes of alteration of micas to kaolinite have been studied by many researchers; e.g., Stoch and Sikora (1976) and Craw *et al.* (1982) studied alteration of micas to kaolinite in weathering and hydrothermal environments, respectively, using X-ray powder diffraction (XRD), electron microprobe analysis, and optical microscopy, and showed that the alteration occurred through fine-scale intergrowths of micaceous phases and kaolinite. Banfield and Eggleton (1988) investigated the processes of weathering of biotite to vermiculite and kaolinite (occurring in granodiorites) using transmission electron microscopy (TEM) and imaged alteration textures at high resolution. They suggested that the biotite-vermiculite and biotite-kaolinite transitions proceeded via direct structural modification and epitaxial crystallization, respectively. Banfield and Eggleton (1990) also described epitaxial replacement of pre-existing illite and smectite by kaolinite that formed by weathering of muscovite. Ahn and Peacor (1987) studied hydrothermal kaolinitization of biotite in a mica schist and proposed that the alteration mechanism involved dissolution of biotite and crystallization of kaolinite along linear boundaries in biotite layers that advanced through the biotite layers.

Ahn and Peacor (1987) showed two modes of occurrence of kaolinite formed from biotite: (1) as packets of layers interstratified within biotite, having a thickness of 50–300 Å, and (2) as two-layer units irregularly interlayered within biotite. Termination of two-layer units of kaolinite by single biotite layers was observed, implying a reaction of one biotite layer to two kaolinite layers. Muscovite-kaolinite intergrowths occurred in the same sample but were not studied. The present study therefore focuses on the muscovite-kaolinite transition to determine the mechanism of alteration of muscovite to kaolinite. The alteration of biotite to kaolinite studied by Ahn and Peacor (1987) was noted in one of the samples studied here, providing an ideal opportunity to compare alteration mechanisms of the

[1] Contribution No. 475 from the Mineralogical Laboratory, Department of Geological Sciences, The University of Michigan, Ann Arbor, Michigan 48109.

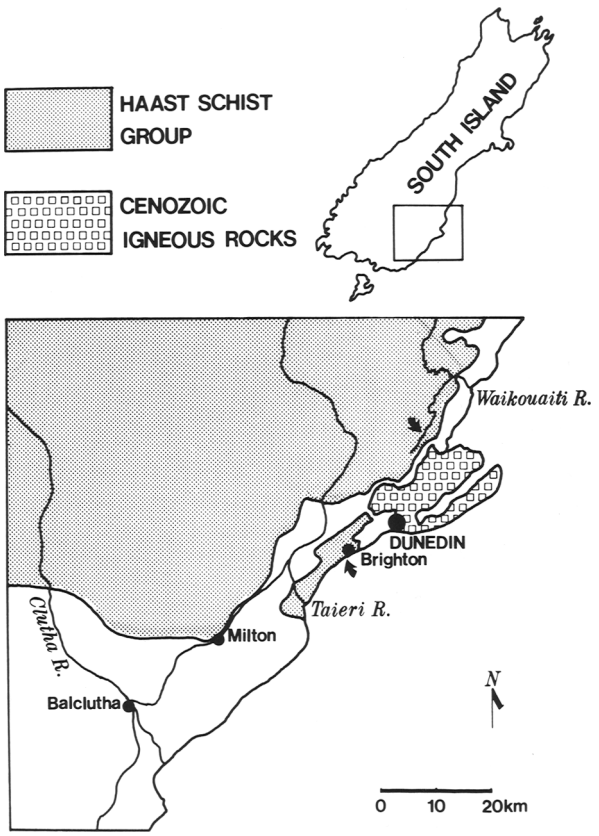

Figure 1. Geological map of the sample localities near Dunedin, New Zealand.

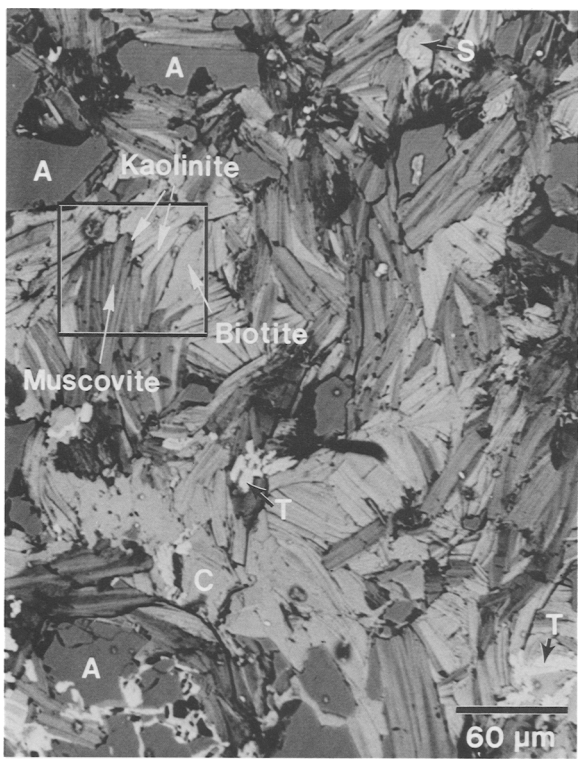

Figure 2. Scanning electron microscope image of mica schist, sample OU37658, from Brighton, New Zealand. Kaolinite occurs as an alteration product interstratified with muscovite and biotite. A = albite; C = calcite; S = siderite; T = titanium oxide.

trioctahedral biotite and the dioctahedral muscovite to dioctahedral kaolinite and to determine if the difference in chemistry of the reactants affected the process.

EXPERIMENTAL

Materials

The principal sample studied, OU37658, was a partially kaolinitized mica schist collected at Brighton, New Zealand, from biotite-grade metapelites of textural zone IV of the Haast Schist (Turner, 1935; Hutton and Turner, 1936). The locality of the sample is illustrated in Figure 1. Kaolinitization of biotite and muscovite in the sample was studied by Craw *et al.* (1982) principally through XRD and electron microprobe data. They described interleaved intergrowths of kaolinite-biotite and kaolinite-muscovite that were resolved only with difficulty by optical microscopy. A scanning electron microscope (SEM) image of the sample is shown in Figure 2 to illustrate the textural relationships. Craw *et al.* (1982) also suggested that the alteration must have been related to a high activity of CO_2 in the hydrothermal fluid, resulting in the partial loss of epidote and the formation of rutile and/or anatase with the consumption of sphene, without oxidation of siderite. A second specimen, OU41794 was a highly kaolinitized mica schist from the area of the South Waikouaiti River, north of Dunedin, New Zealand (Figure 1). Both samples were kindly supplied by D. Craw and D. S. Coombs of the University of Otago, New Zealand.

Methods

Thin sections were prepared having an orientation approximately normal to the well-developed crenulated schistosity so that (001) planes of the micas were preferentially oriented normal to the section. Thin sections were examined by optical microscopy and SEM to select areas containing abundant muscovite-kaolinite aggregates for TEM preparation. Aluminum washers were attached to the selected areas and detached from the thin section. The washer specimens were then ion-milled and carbon-coated for TEM observation.

The samples were examined using three different scanning-transmission electron microscopes (STEMs), including JEOL JEM-100CX, JEOL 2000FX, and Philips CM12 instruments, operated at 100, 200, and 120 kV, respectively. X-ray energy-dispersive spectrometry (EDX) analyses were carried out at an emission current of ~10 μA in the CM12 STEM using a low-angle Kevex Quantum detector and computer system, by tilting the specimen holder about 20° toward

https://doi.org/10.1346/CCMN.1991.0390101 Published online by Cambridge University Press

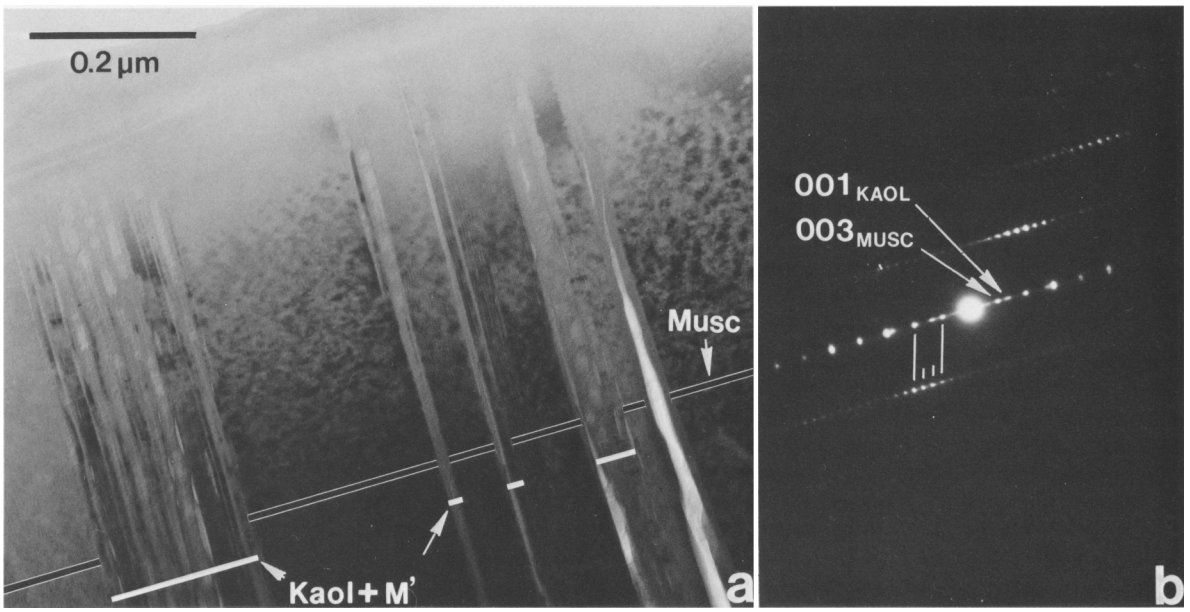

Figure 3. (a) Transmission electron microscope image of interstratified muscovite and kaolinite. M1′ symbolizes a micaceous phase other than muscovite. (b) Electron diffraction pattern of (a) showing reflections of kaolinite and a three-layer polytype of muscovite.

the detector (34° X-ray take-off angle), using the scanning mode. Thin-film conditions (Lorimer and Cliff, 1976) were assumed for quantitative analyses, using albite (Na, Al), clinochlore (Mg, Al, Fe), synthetic fayalite (Fe), muscovite (K, Al), rhodonite (Mn, Fe, Ca), and sphene (Ti, Ca) as standards.

Most data presented here were obtained with the Philips CM12 STEM. Lattice-fringe images were obtained with a condenser aperture of 70-μm and an objective aperture of 70-μm diameter, so as to include the 003 reflection of muscovite. A magnification of 45,000× and minimum brightness were commonly used to minimize beam damage of the specimens. Electron diffraction patterns were obtained using a selected-area aperture 10 μm in diameter. Optical diffraction patterns were derived from TEM images using an optical bench system.

In the present study, the terminology used for various units of crystal structure follows the recommendations of the Nomenclature Committee of The Clay Minerals Society (Bailey *et al.*, 1971) and the Association International pour l'Étude des Argiles (AIPEA, Brindley and Pedro, 1972; Bailey, 1980).

RESULTS

Metamorphic muscovite

Muscovite generally was noted as thick packets of layers interstratified with kaolinite layers, with a total stack thickness of a few hundred Ångstroms to ~30 μm (Figures 2 and 3). Electron diffraction patterns suggest that most of the muscovite consisted of a two-

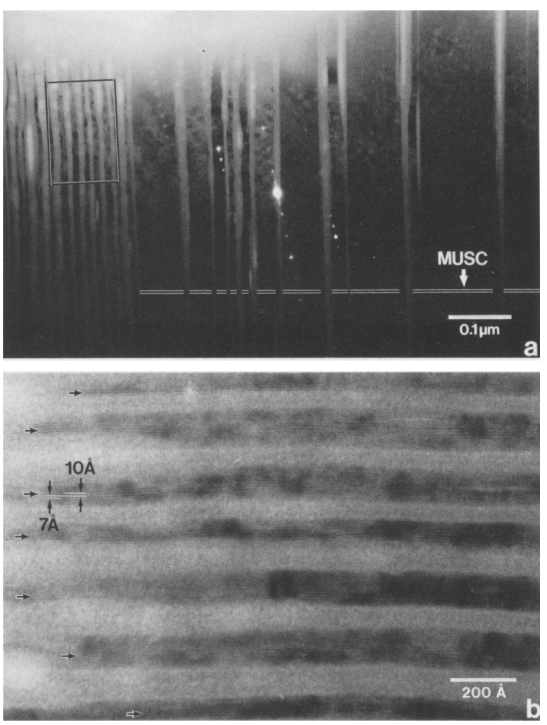

Figure 4. (a) Transmission electron microscope image and electron diffraction pattern of kaolinitized muscovite. Unlined areas are kaolinite packets interstratified with a smectite-like phase. (b) Lattice-fringe image of the area outlined with a square in (a), showing interstratification of kaolinite and smectite-like layers (marked by black arrows).

https://doi.org/10.1346/CCMN.1991.0390101 Published online by Cambridge University Press

Table 1. Analytical electron microscope and electron microprobe analyses of muscovite in the hydrothermally altered mica schist at Brighton, New Zealand.[1,2,3]

	1	2	3	4	5	6	7	8	9
Si	6.61 (0.14)	6.60 (0.14)	6.62 (0.14)	6.58 (0.14)	6.56 (0.14)	6.48 (0.11)	6.45 (0.11)	6.64	6.40
Al(IV)	1.39 (0.04)	1.40 (0.04)	1.38 (0.04)	1.42 (0.04)	1.44 (0.04)	1.52 (0.03)	1.55 (0.03)	1.36	1.60
Al(VI)	2.94 (0.08)	2.95 (0.08)	2.89 (0.08)	2.94 (0.08)	3.04 (0.09)	3.03 (0.06)	3.00 (0.06)	2.83	3.13
Ti	0	0.02 (0.01)	0.02 (0.01)	0	0	0.02 (0.01)	0	0.01	0.01
Fe	0.34 (0.03)	0.33 (0.03)	0.34 (0.03)	0.33 (0.03)	0.30 (0.02)	0.37 (0.02)	0.38 (0.02)	0.49	0.40
Mg	0.72 (0.06)	0.70 (0.06)	0.75 (0.06)	0.73 (0.06)	0.65 (0.05)	0.58 (0.04)	0.62 (0.04)	0.66	0.46
Ca	0.04 (0.01)	0	0.04 (0.01)	0	0	0	0	0	0
Na	0.15 (0.03)	0.18 (0.04)	0.22 (0.05)	0.14 (0.03)	0.15 (0.03)	0.14 (0.03)	0.18 (0.03)	0.06	0.05
K	1.56 (0.06)	1.63 (0.06)	1.66 (0.07)	1.70 (0.07)	1.40 (0.06)	1.36 (0.04)	1.12 (0.04)	1.68	1.23
Al/Si	0.66	0.66	0.65	0.66	0.68	0.70	0.71	0.63	0.74
Mg/Fe	2.12	2.12	2.21	2.21	2.17	1.57	1.63	1.35	1.15

[1] Normalization is based on total of 12 tetrahedral and octahedral cations and all Fe assumed to be ferrous.
[2] Columns 1–4 and 5–7 are analyses of unaltered and partially altered muscovite, respectively. Columns 8 and 9 are recalculated from electron microprobe analyses of Craw *et al.* (1982).
[3] Number in parentheses indicates two standard deviations based on counting statistics.

layer polytype, but with three-layer polytypism occurring uncommonly (e.g., Figures 3 and 4). Both polytypes were partially kaolinitized. AEM analyses indicate that the muscovite was phengitic in composition, having an Al/Si ratio of ~0.65 and a Mg/Fe ratio of ~2.1–2.2 (analyses 1–4 in Table 1). These values are very nearly equal to those of the microprobe analysis (analysis 8 in Table 1) of Craw *et al.* (1982). Some analyses (AEM analyses 5–7 and microprobe analysis 9 in Table 1) have a relatively low alkali content that cannot be attributed to interference by kaolinite alone. As shown below, the presence of a second micaceous phase (smectite and/or illite?) may also have contributed to such anomalous phengitic compositions.

Kaolininte

Kaolinite was noted as packets of layers about 100–600 Å in thickness (Figures 3 and 4). Kaolinite was very readily damaged by the electron beam, with image details, such as lattice fringes, and electron diffraction patterns, being lost in only a few seconds. It was, however, very different in appearance from muscovite (e.g., Figures 4, 5, and 7), so that even if lattice fringes were not observed because of beam damage, the occurrence of kaolinite was readily affirmed. Kaolinite was also characterized by decrease in intensity and increase in diffuseness of reflections with increasing time of exposure to the electron beam. In the areas directly adjacent to muscovite packets, kaolinite packets more commonly retained their layer structure in lattice-fringe images, as was also observed by Ahn and Peacor (1987) for biotite-kaolinite intergrowths.

The kaolinite was commonly highly disordered in stacking sequence in areas in which kaolinite occurred as relatively thin packets of layers (~100 Å), interstratified with wavy micaceous layers, as suggested by diffuseness parallel to c* in non-00*l* reflection rows with $k \neq 3n$ electron diffraction patterns (e.g., Figure 5). Where kaolinite formed relatively thick packets of layers within which micaceous layers were relatively straight and rare or absent, however, kaolinite displayed reflections of an ordered one-layer polytype (e.g., Figures 6 and 7). The ordered polytype was especially common in the highly kaolinitized rocks found near the South Waikouaiti River north of Dunedin (Figure 1). EDX analyses show that the kaolinite domains have a range of Mg/Fe ratios, which was far smaller than that of the primary muscovite, and a maximum Al/Si ratio of 0.84 (Table 2). The anomalously low Al/Si ratios suggest some contamination from micaceous phase(s).

Figure 6a shows a large area of kaolinite that consists of many packets of layers, each of which is ~500–600 Å thick. Some packets of layers consist of several "subpackets," which are separated by parallel layers having distinctly different contrast (Figure 6d). No micaceous (i.e., 10-Å) layers were observed in such areas. The corresponding electron diffraction pattern (Figure 6b) shows closely spaced reflections in addition to reflections of a one-layer polytype of kaolinite in both the 00*l* and 21*l* reflection rows. Such reflections were not noted where the contrast features defining the "subpackets" were absent. The reflections were therefore inferred to be related to the "subpackets" seen in the lattice-fringe image (Figure 6d). This inferrence is also suggested by the optical diffraction patterns (e.g., Figure 6c) that suggest that closely-spaced periodic 00*l* reflections were derived solely from the areas containing "subpackets." Such reflections are probably due to mixed-layering of structurally/chemically distinct kaolinite layers, although the possible contribution of polytypism cannot be entirely excluded.

Other micaceous phases

Lattice fringes having a spacing of ~10 Å and assumed to correspond to mica-like 2:1 layers were very

https://doi.org/10.1346/CCMN.1991.0390101 Published online by Cambridge University Press

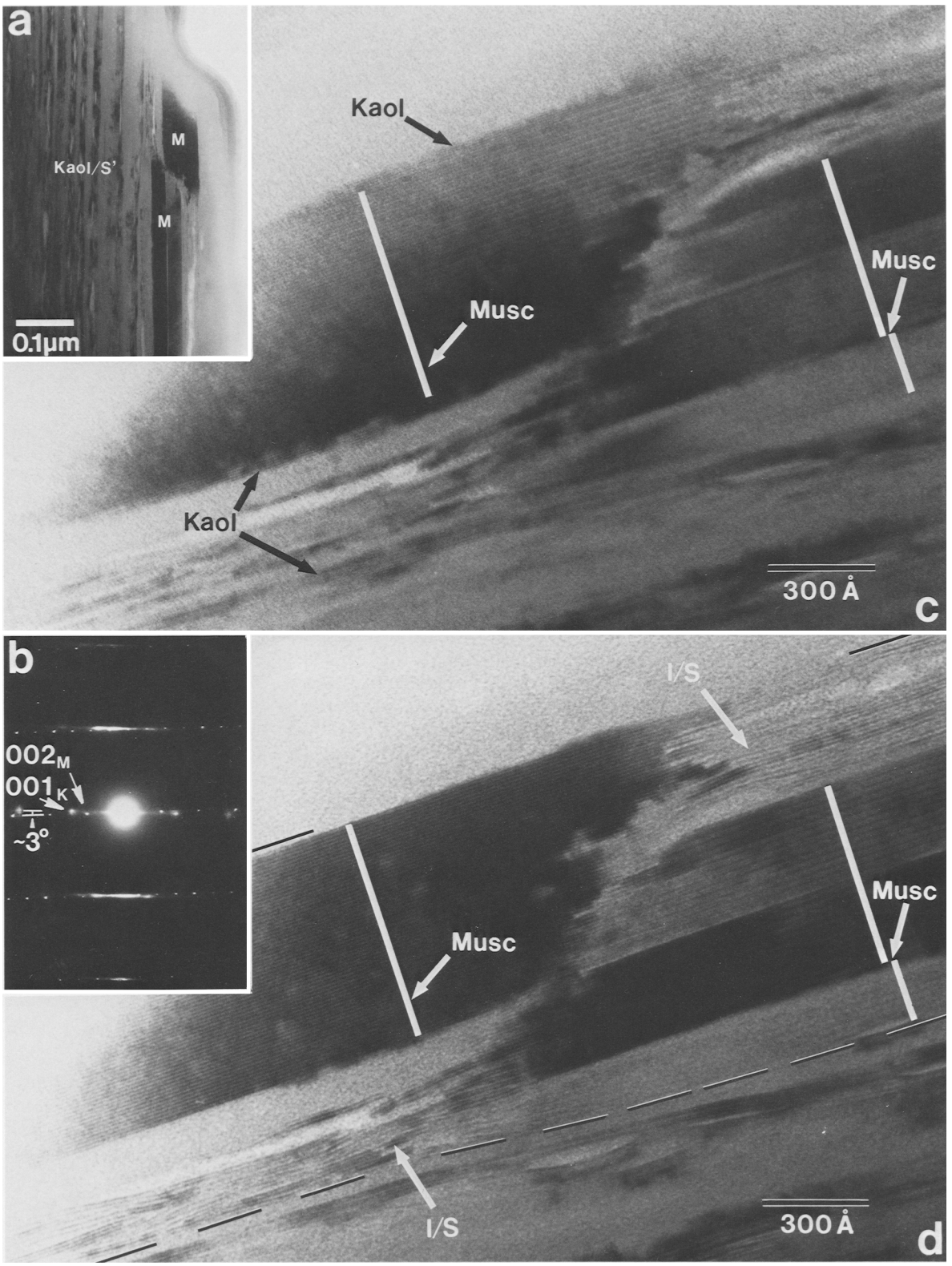

Figure 5. (a) Transmission electron microscope image of interstratified packets of kaolinite and smectite-like layers (Kaol/S') and primary muscovite (M); (b) electron diffraction pattern of (a) showing superimposed reflections of a two-layer polytype of muscovite and disordered kaolinite, including 11*l* reflections of muscovite and 11*l* or 02*l* reflections of kaolinite; (c) lattice-

https://doi.org/10.1346/CCMN.1991.0390101 Published online by Cambridge University Press

Table 2. Analytical electron microscope analyses of kaolinite in the hydrothermally altered mica schist at Brighton, New Zealand.[1,2,3]

	1	2	3	4	5	6	7	8
Si	4.23 (0.08)	4.24 (0.08)	4.28 (0.10)	4.44 (0.11)	4.46 (0.10)	4.45 (0.11)	4.52 (0.09)	4.77 (0.11)
Al	3.57 (0.08)	3.54 (0.08)	3.45 (0.10)	3.25 (0.10)	3.28 (0.09)	3.23 (0.10)	3.30 (0.08)	3.06 (0.09)
Ti	0	0	0	0	0.01 (0.01)	0	0	0
Fe	0.11 (0.01)	0.11 (0.01)	0.16 (0.01)	0.23 (0.02)	0.13 (0.01)	0.22 (0.02)	0.10 (0.01)	0.08 (0.01)
Mg	0.09 (0.02)	0.11 (0.02)	0.11 (0.02)	0.08 (0.02)	0.11 (0.02)	0.10 (0.02)	0.07 (0.01)	0.09 (0.02)
Ca	0	0	0	0.02 (0.01)	0.04 (0.01)	0	0	0.02 (0.01)
Na	0.05 (0.01)	0	0.08 (0.02)	0.10 (0.03)	0.07 (0.02)	0.09 (0.02)	0.10 (0.03)	0
K	0.04 (0.01)	0.03 (0.01)	0.04 (0.01)	0.06 (0.01)	0.06 (0.01)	0.05 (0.01)	0.03 (0.01)	0.04 (0.01)
Al/Si	0.84	0.83	0.81	0.73	0.74	0.73	0.73	0.64
Mg/Fe	0.82	1.00	0.69	0.35	0.85	0.45	0.70	1.13

[1] Normalization is based on total of 8 tetrahedral and octahedral cations and all Fe assumed to be ferrous.
[2] Column numbers represent analyses from different kaolinite areas containing micaceous layers.
[3] Number in parentheses indicates two standard deviations based on counting statistics.

common in packets of kaolinite layers. The mica-like phase(s) commonly occurred as packets of 1 to ~10 straight or wavy layers (Figures 4, 5, and 7). AEM data for mixtures of this phase(s) and kaolinite and muscovite (Table 2 and analyses 5–7 in Table 1) have low alkali contents inconsistent with Al/Si and Mg/Fe ratios for mixtures of muscovite + kaolinite. The plots of Mg/Fe ratios and numbers of interlayer cations vs. Al/Si ratios of the data from Tables 1 and 2 are shown in Figures 8a and 8b, respectively. The numbers of interlayer cations for impure kaolinite (analyses from Table 2) are recalculated based on a total of 12 cations in tetrahedral and octahedral sites as for muscovite. The illustrations show that some of the data do not fall on the tie line between the unaltered muscovite and ideal kaolinite, assuming no interlayer cations and an extremely small Mg/Fe ratio for kaolinite (plotted in the lower-right corner). The bias of the distribution of the data indicates the presence of at least a third phase having a smaller Mg/Fe ratio and interlayer content and a smaller Al/Si ratio relative to the phengitic muscovite and kaolinite, respectively. The low alkali contents and Al/Si ratios of the micaceous phase(s) relative to muscovite are consistent with an identification of either smectite or illite. Craw *et al.* (1982) also observed abnormally low K values in their muscovite analyses for the same specimen as used in the present study (e.g., analysis 9 in Table 1). They suggested that the low K values of "muscovite" may result from loss of K due to alteration of muscovite to illite or "hydromica." A similar micaceous phase was also observed in kaolinite of weathering origin by Lee *et al.* (1975) and Banfield and Eggleton (1990) using TEM. Such a phase(s), thus, apparently is commonly associated with the mica-to-kaolinite transition.

From a textural point of view, the wavy layers (termed smectite-like phase or layers, hereafter) were similar in appearance to smectite observed in other studies (e.g., Ahn and Peacor, 1986; Bell, 1986; Klimentidis and Mackinnon, 1986; Yau *et al.*, 1987; Jiang *et al.*, 1990), the lens-shaped pores occurring as layer separations caused by beam damage. The curvature in lattice-fringes is diagnostic of smectite (Figure 5). On the other hand, the straight layers are most likely illite (Figure 7), by analogy with images observed in the papers referred to above. The presence of an expandable smectite-like phase was not indicated by XRD patterns of the bulk rock of sample OU37658 (Craw *et al.*, 1982), probably because the amount of the phase was too small. Smectite, described as a product of hydrothermal or weathering alteration, however, was detected by XRD in samples from other localities of the Haast Schist subjected to the hydrothermal alteration (Craw *et al.*, 1982). The smectite (or I/S) noted in the present study probably was a product of hydrothermal alteration because of the presence of intimate intergrowths of smectite with kaolinite and no indication of oxidation of the siderite in the sample. "Degraded muscovite," a term that has often been used to describe altered muscovite containing anomalously low K, is thus likely a mixture of different micaceous phases, such as muscovite, illite, and smectite.

Structural and textural relationships between kaolinite and micaceous phases

Where packets of kaolinite and micaceous layers alternate, the boundaries between them were typically defined by parallel lattice fringes having no strain contrast (e.g., Figures 5 and 7). Low-angle boundaries between kaolinite and muscovite crystals were not observed. Electron diffraction patterns of intergrown muscovite and kaolinite commonly showed parallelism of 00*l* reflection rows of both phases. These rela-

←
fringe image of the muscovite area in (a) with packets of muscovite layers denoted by white bars; (d) lattice-fringe image of the same area as (c) but tilted a few degrees with respect to (c).

https://doi.org/10.1346/CCMN.1991.0390101 Published online by Cambridge University Press

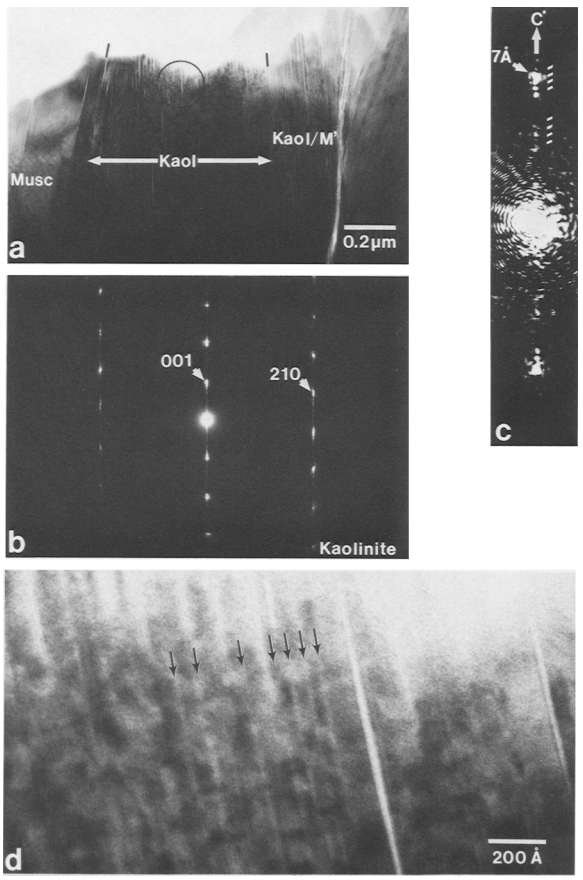

Figure 6. (a) Transmission electron microscope image of relatively thick packets of kaolinite coexisting with muscovite and interstratified kaolinite and mica-like layers (Kaol/M'); (b) electron diffraction pattern of (a) showing reflections of an ordered one-layer polytype of kaolinite associated with closely spaced reflections within 00*l* and 21*l* reflection rows; (c) optical diffraction pattern of the marked area in (d) showing closely spaced 00*l* reflections; (d) lattice-fringe image of the circled area in (a) showing "subpackets" of kaolinite layers separated by kaolinite layers with different contrast (marked by black arrows).

tions are consistent with, but do not prove coherent phase boundaries.

Figure 7 shows thin packets of straight 10-Å layers interstratified with kaolinite layers and separated by approximately equal numbers of kaolinite layers. The electron diffraction pattern (Figure 7b) shows very closely spaced reflections along c*, in addition to normal 00*l* reflections of kaolinite. Non-00*l* reflections are not present. The pattern of closely spaced reflections is somewhat complex and appears to be a combination of several sets of reflections having different periodicities. Figures 7d and 7e are lattice-fringe images of part of Figure 7a (labeled d and e) showing alternation of kaolinite and micaceous-layer units having a periodicity on the order of ~200–300 Å. Optical diffraction patterns (Figure 7f) of the circled areas in Figure 7a suggest that the whole area consists of several domains, each of which gave rise to a different periodicity in the electron diffraction patterns. The interstratification was thus sufficiently regular to have given rise to a periodic diffraction pattern. Interestingly, the damaged and undamaged elongate areas also appear to alternate regularly with each other, perhaps contributing to the closely spaced reflections in the diffraction patterns. Figure 7c is the electron diffraction pattern from the area including the kaolinite and adjacent muscovite in Figure 7a, obtained after tilting the specimen a few degrees in order to observe non-00*l* reflections. This pattern shows that the kaolinite and muscovite are one-layer and two-layer polytypes, respectively, and that 00*l* and 11*l* reflection rows of both kaolinite and muscovite are parallel to each other.

Smectite-like layers were observed to be interstratified only with kaolinite, but not with muscovite; i.e., the smectite-like phase did not share (001) boundaries with mica. Transition boundaries along layers between kaolinite and muscovite and the smectite-like phase were not detected, but "along-layer" transitions between muscovite and the smectite-like phase were rarely observed, as shown in Figure 5d. Here, the smectite-like phase occurs as packets of wavy layers and displays periodic layer contrast with ~20-Å periodicity over short distances, implying that this phase could be mixed-layer illite-smectite (I/S) with R1 ordering; i.e., ISIS . . . (Guthrie and Veblen, 1989; Veblen *et al.*, 1990). The corresponding electron diffraction pattern (Figure 5B) shows weak streaking along c*, which could have been caused by disorder in the R1-ordered sequence. This streaking is not a clear indication of the presence of I/S, however, because of possible double diffraction derived from the streaking nearly parallel to c* of muscovite in non-00*l* reflection rows ($k \neq 3n$) of disordered kaolinite. Qualitative EDX data, however, suggest that this phase had a low alkali content and Al/Si ratio relative to muscovite that can not be accounted for solely by contamination by kaolinite, consistent with the identification of the wavy layers as I/S.

Figures 5c and 5d show three packets of muscovite layers (marked with white bars), which are parallel to each other, having different contrast presumably due to slightly different orientations. The upper two packets appear to have some continuous layers in common, implying that they might have originally consisted of a single packet that was deformed due, for example, to tectonic stress during metamorphism. In Figure 5d, the stack thickness decreases from right to left, which corresponds to a progression from a stack consisting of muscovite + smectite-like phase at the upper-right to muscovite + kaolinite + smectite-like phase at the lower-left. This texture suggests that a volume loss was involved in the transition from muscovite to the smectite-like phase + kaolinite assemblage. The kaolinite layers appear to be terminated against the smectite-

https://doi.org/10.1346/CCMN.1991.0390101 Published online by Cambridge University Press

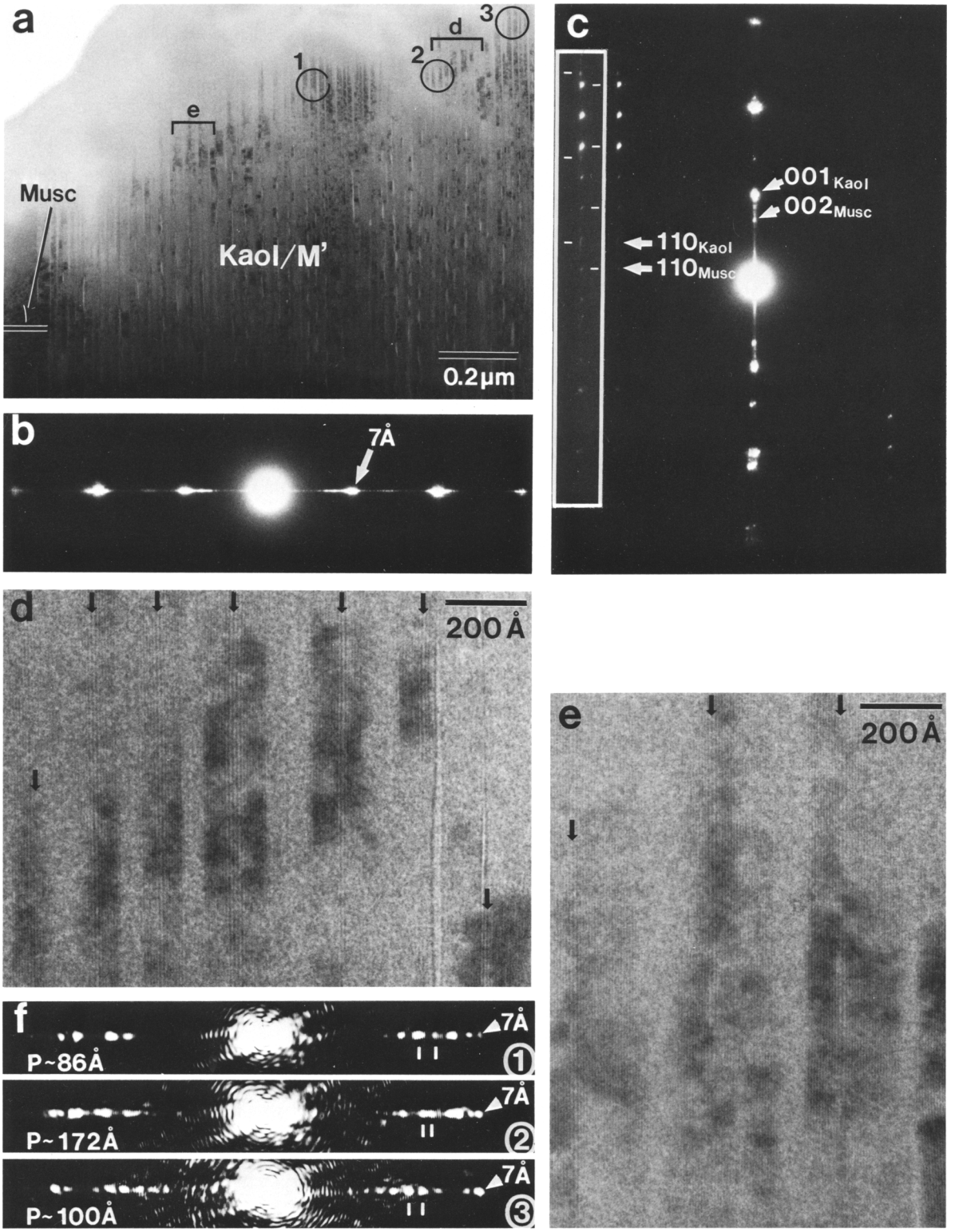

Figure 7. (a) Transmission electron microscope image of interstratified kaolinite and micaceous layers (Kaol/M'); (b) electron diffraction pattern of (a) showing closely spaced 00*l* reflections; (c) electron diffraction pattern of the area close to the muscovite crystal in (a), showing orientation relationship between muscovite and adjacent kaolinite; (d) and (e) are lattice-fringe images of the labeled areas (d and e) in (a), showing periodic interstratification of kaolinite and micaceous layers. (f) Optical diffraction patterns of circled areas (1, 2, and 3) in (a) showing variable periodicities of interstratification.

https://doi.org/10.1346/CCMN.1991.0390101 Published online by Cambridge University Press

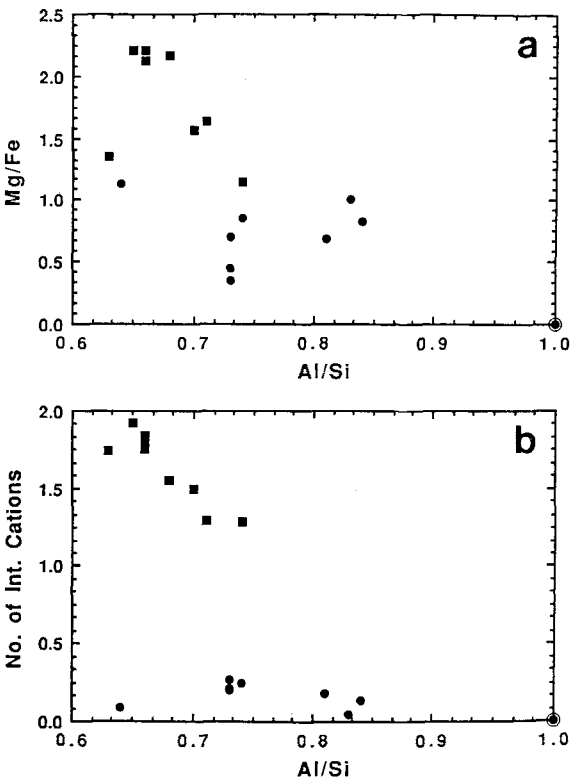

Figure 8. Plots of (a) Al/Si ratios vs. Mg/Fe ratios and (b) Al/Si ratios vs. numbers of interlayer cations of muscovite and kaolinite. The numbers of interlayer cations were calculated based on a total of 12 tetrahedral and octahedral cations for both muscovite and kaolinite. ■ = data from Table 1; ● = data from Table 2; ◉ = ideal kaolinite, assuming no interlayer cations and an extremely small Mg/Fe ratio.

like phase instead of muscovite, without continuation along layers, as in a low-angle grain boundary. Thus, the kaolinite and smectite-like layers apparently grew independently within different areas of muscovite, with different orientations. The electron diffraction pattern (Figure 5b) shows that the 11*l* row of muscovite and the 11*l* or 02*l* rows of disordered kaolinite are superimposed, but at an angle of about 3°. The non-parallelism of 00*l* reflection rows of muscovite and kaolinite implies non-parallelism of their 001 lattice fringes. The lattice fringes of muscovite and kaolinite, however, were in all other areas of the sample observed to be parallel to each other at the interfaces (Figure 5c), implying that the non-parallelism is due to primary growth of adjacent muscovite crystals that here grew with low-angle boundaries.

DISCUSSION

Summary of observations of kaolinitization of muscovite

Kaolinitization of muscovite resulted in interstratification of packets of muscovite and kaolinite, but no transition boundaries along layers were observed. Kaolinite packets consisted of at least 10 layers that were invariably parallel to adjacent 2:1 layers of muscovite or a smectite-like phase, with no strain contrast at interfaces. Parallelism of 00*l* rows and overlapping of 11*l* rows of both kaolinite and muscovite showed that the reaction was topotaxial. These relations are consistent with, but do not prove that interfaces were coherent. Kaolinite packets interstratified with micaceous phases were ordered to the extent that periodicity was observed in electron diffraction patterns. Kaolinite was commonly disordered, occurring as thin packets of layers interstratified with packets of smectite-like layers. Electron diffraction patterns contained reflections derived from ordering of the thickness and frequency of occurrence of smectite-like layers. Ordered kaolinite occurred as relatively thick packets of layers, within which interstratified straight micaceous layers were rare or absent. Muscovite and smectite-like layers did not appear to share boundaries parallel to (001), but transitions along 001 layers from muscovite to a smectite-like phase were observed rarely.

Alteration mechanism

Many chemical reactions can be written for the alteration of muscovite to kaolinite, differing primarily in whether or not volume decreases, is unchanged, or increases. Two types of replacement mechanism for the transition from 2:1 phyllosilicates, such as muscovite and phlogopite, to 1:1 phyllosilicates, such as kaolinite and serpentine, have been proposed (Stoch and Sikora, 1976; Sharp *et al.*, 1990) based on considerations of minimum volume and chemical changes. Stoch and Sikora (1976) suggested a transition of two muscovite layers to three kaolinite layers, involving the formation of interlayer gibbsite-like sheets and inversion of tetrahedral sheets:

$$2\ \underset{\text{muscovite}}{K_2Al_4(Si_6Al_2)O_{20}(OH)_4} + 6\ H_2O + 4\ H^+$$

$$= 3\ \underset{\text{kaolinite}}{Al_4Si_4O_{10}(OH)_8} + 4\ K^+.$$

This reaction minimizes chemical change (gain only of H^+ and H_2O and los of K^+), but involves a small increase in volume (eight anion planes are replaced by nine anion planes). Sharp *et al.* (1990) proposed a mechanism involving the transition of three 2:1 layers to four 1:1 layers for the phlogopite-to-serpentine transition which, if applied to the dioctahedral phases of this study is equivalent to:

$$3\ \underset{\text{muscovite}}{K_2Al_4(Si_6Al_2)O_{20}(OH)_4} + 20\ H^+$$

$$= 4\ \underset{\text{kaolinite}}{Al_4Si_4O_{10}(OH)_8} + 2\ Si^{+4} + 2\ Al^{+3} + 6\ K^+.$$

This reaction minimizes stress due to volume change, because the structures are based on closest-packing (to

https://doi.org/10.1346/CCMN.1991.0390101 Published online by Cambridge University Press

a first approximation) and the number of anions and anion planes is unchanged. Even though no direct evidence exists for either of the reactions given above, these reactions serve as approximations of the actual mechanisms. They also point out that although the relative change in proportions of anions and cations is small, significant structural reorganization must occur, and a fluid must be present to account for transport of reactants and products.

The transition of muscovite to kaolinite minimally involves the removal of interlayer alkali ions and octahedral Mg and Fe, replacement of tetrahedral Al by Si, reorientation of the Si tetrahedra in one of two sheets, formation of one new dioctahedral sheet, and gain of water and/or protons (H^+) to form OH groups coordinating Al (assuming an ideal kaolinite composition). The flux of cations depends on the relative number of layers retained; e.g., Si must be added to the system if the number of tetrahedral sheets is unchanged. The alteration process thus requires substantial local diffusion of cations, including Si and tetrahedrally coordinated Al, disruption of bonds in all sheets, and addition or loss of cations and/or anions. Such major changes demand at least partial dissolution of octahedral and tetrahedral sheets of the mica structure and the crystallization of kaolinite. Dissolution-crystallization mechanisms for transitions between phyllosilicates under low-temperature conditions have also been suggested in other studies; e.g., Yau *et al.* (1984) for the phlogopite-to-chlorite transition, Ahn and Peacor (1986) and Yau *et al.* (1987) for the smectite-to-illite reaction, Ahn and Peacor (1987) for the biotite-to-kaolinite transition, and Banfield and Eggleton (1988) for biotite-to-vermiculite and/or -kaolinite alteration. Dissolution-crystallization through a fluid medium is required simply because solid-state mechanisms are too sluggish at low temperatures, as in the samples studied here.

The only direct evidence regarding relative change in volume observed in the present study was obtained in images shown in Figure 5; packets of layers consisting of kaolinite plus I/S were found to be thinner than the equivalent part of unaltered muscovite, in which the I/S was continuous "along-layer" with primary muscovite. Direct evidence from other studies, consisting of lattice-fringe images containing transition boundaries, generally is not consistent with a simple constant-volume relation. For example, Ahn and Peacor (1987) demonstrated that the transition of one biotite layer to two kaolinite layers resulted in a substantial volume increase and misfit of (001) boundaries. Veblen and Ferry (1983) and Olives and Amouric (1984) described the transitions of two biotite layers to one chlorite layer and one biotite layer to one chlorite layer, respectively, resulting in a large volume loss and gain, respectively. In a study of the phlogopite-to-chlorite transition, Yau *et al.* (1984) showed that both volume loss and gain can occur locally and suggested that they may compensate for each other in volume change on a larger scale, as was also suggested by Veblen and Ferry (1983). Nearly "equal-volume" reactions are rare but do exist, e.g., Yau *et al.* (1984) described a single example of a transition of 14 phlogopite layers to 10 chlorite layers. A summary of observed relationships thus implies that, at least on a local scale, phyllosilicate alteration mechanisms may involve relatively large changes in volume, but that no general rule exists regarding conservation of volume.

The results of the present study suggest a direct transition from muscovite to either kaolinite or a 2:1 phase. Such direct transitions of one phyllosilicate to another without the formation of an intermediate phase have often been observed (e.g., Veblen and Ferry, 1983; Olives and Amouric, 1984; Ahn and Peacor, 1987; Banfield and Eggleton, 1988). Indeed, this relation is true for all such transitions of which the present authors are aware. Alteration of other silicates having non-phyllosilicate polymerization schemes to form phyllosilicates, however, has often been reported to occur via formation of intermediate materials, such as a noncrystalline phase or some other metastable phase (e.g., Eggleton and Buseck, 1980; Eggleton and Boland, 1982; Eggleton, 1984; Banfield and Eggleton, 1990). In other words, even though the alteration of muscovite to kaolinite requires major reorganization of virtually all elements of the structure, including major change in chemistry of the tetrahedral sheets, the products and direct reactants share a common polymerization scheme. This reactant-product relation implies that the dissolution-crystallization process may involve retention of at least part of the polymerized units, or that the general similarity in reactant and product layers provides easy pathways for change. This relation is also consistent with a general kinetically controlled Ostwald step-rule relation, in which if structural differences between reactant and product are large, intermediate phases will form.

Kaolinite was noted only as thick packets of layers in the present study. Small numbers of kaolinite layers within muscovite were never observed, implying that alteration was by multiple-layer replacement. Inasmuch as all observed interfaces were parallel to layers of kaolinite and muscovite (no layer terminations against one another), alteration must have proceeded along layers, as noted by Ahn and Peacor (1987). In addition, alteration fronts must have been self-perpetuating and proceeded rapidly along layers relative to the rate of initiation of alteration of a given layer(s), once they were initiated within 2:1 layers at crystal edges or strained areas, because "along-layer" transitions were not observed. In the case of the alteration of biotite to kaolinite occurring in the same specimen as the source of most observations of this study, alteration was inferred to occur across "along-layer" in-

terfaces between reactant and products, because "along-layer" interfaces were observed (Ahn and Peacor, 1987). Such one-dimensional discontinuities in structure may have served as pathways for fluids carrying reactant and product ions. Although interfaces were not directly observed in this study, the lack of "across-layer" transitions is compatible with a similar mechanism. Such an advancing alteration front would be self-perpetuating only along the layers within which the polymerization scheme was breached, once it was initiated. Boundaries between primary phlogopite and secondary serpentine were likewise noted by Sharp *et al.* (1990) to be always parallel to (001), consistent with an alteration process similar to that of the muscovite-to-kaolinite alteration. The analogy between the di- and tri-octahedral reactant-product pairs implies a close relationship between alteration processes and reactant-product relations.

Ahn and Peacor (1987) showed that the terminations of one mica layer by two kaolinite layers occurred in the alteration of trioctahedral biotite to dioctahedral kaolinite, which were not observed in the present study. This may have been because the biotite-to-kaolinite alteration requires greater chemical adjustment and, therefore, greater ion and fluid fluxes than does the muscovite-to-kaolinite alteration. Termination of reaction fronts may have been more likely in the biotite-to-kaolinite alteration in areas where the supply of fluid was insufficient or changed abruptly.

Order-disorder of kaolinite and ordering of interstratification

The presence of long-range ordering in thickness and periodicity of both the packets of kaolinite within muscovite and the variable contrast in 7-Å layers, is unusual, especially to the extent that it gives rise to periodicity in diffraction patterns. Although regions in which the distribution of kaolinite packets appeared to be random, some degree of order was the rule rather than the exception. The periodicity seems to be especially meaningful in that Sharp *et al.* (1990) observed the same feature in the chemically different phlogopite-serpentine system. Although direct evidence for a cause was not observed, the periodicity was probably due either to preferential alteration of periodically strained layers of muscovite that developed before alteration, or to stress developed during alteration.

Evidence exists that replacement of layers of one phyllosilicate by layers of another gives rise to local stress if the layer thicknesses are different, the effects of which can cause periodicity in the distribution of altered layers. Banfield and Eggleton (1988) studied the transformation of biotite to vermiculite and documented the replacement of single layers of biotite by single layers of vermiculite. They showed that the local stress induced at the end of one newly formed vermiculite layer at the "along-layer" transition boundary with biotite promoted growth of vermiculite layers in the opposite direction, giving rise to alternating layers of biotite and vermiculite. Ahn and Peacor (1987) observed similar ordering over very short distances, in which two layers of kaolinite replaced single layers of biotite. Because the periodicities observed in the present study occurred over layer thicknesses of tens or hundreds of Ångstroms, such a mechanism seems highly unlikely.

Periodicity produced by preferential alteration of periodically strained layers is an alternative possibility. Jiang *et al.* (1990) showed that alteration of muscovite to I/S preferentially took place in domains that had been preferentially strained. The strain, consisting in part of deformed layers, was inferred to be due to stress developed either during sediment compaction or during tectonic activity. Unpublished data from the authors' laboratory suggest that vermiculite preferentially replaced strained layers of Ti-phlogopite in a Mn-rich quartzite. Well-defined crenulation in rock fabric and preferred orientation of phyllosilicates reflect the syn-metamorphic tectonic stress that affected the samples studied here. Although we are aware of no studies showing that periodic strain may arise in mica grains subjected to such stress, the occurrence of periodic alteration suggests that the possible existence of such relations should be investigated.

The cause of the periodicity in contrast within layers having 7-Å periodicity is also not clear. The individual packets having different contrast are too small to be resolved by EDX and electron diffraction. In addition, no chemical differences are apparent between areas that have periodic contrast and areas that contain homogeneous contrast, although superstructure reflections were observed in the former areas. The cause of periodic contrast within kaolinite packets is therefore unresolved. Nevertheless, the occurrence of superperiodicities in the distribution of kaolinite and micaceous layers in the same samples suggests a common cause.

A specific distribution in polytypism of kaolinite has also been noted: stacking sequences of layers interstratified with smectite-like layers were random, whereas those interstratified with or not interstratified with illite or muscovite layers were ordered. Ordered kaolinite was generally more stable in the electron beam than was disordered kaolinite. No explanation for these relations can be offered, but they are described for the record.

Formation relations between muscovite, kaolinite, and the smectite-like phase

Alteration of white micas to smectite-like phases + kaolinite has been observed in many studies, with smectite generally appearing to have formed prior to kaolinite. The commonly observed sequence is: muscovite → illite (sericite) → mica/smectite phases → smectite phase → kaolinite, through complex inter-

https://doi.org/10.1346/CCMN.1991.0390101 Published online by Cambridge University Press

growth of these phases (e.g., Meunier and Velde, 1979; Beaufort and Meunier, 1983; Banfield and Eggleton, 1990). In some samples (e.g., Stoch and Sikora, 1976), kaolinite apparently directly transformed from muscovite, without an intermediate phase.

In the present study, one instance of direct "along-layer" transitions was observed. As shown in Figure 5, I/S layers abut against muscovite layers and coexist with kaolinite. Furthermore, smectite-like layers are commonly interstratified with kaolinite layers (e.g., Figures 4 and 5). These textures imply that smectite, illite, or I/S could have been an intermediate phase in samples in which kaolinite now occurs as a replacement of muscovite. Because kaolinite packets were not observed separated from muscovite by smectite-like layers in all other observations, whether kaolinite generally formed as a direct alteration product of muscovite or if a "degraded" 2:1 phase served as an intermediate phase cannot be determined.

Meunier and Velde (1979) studied the weathering process of two-mica granites and suggested that chemical forces that produce new minerals are commonly constrained to small volumes, often on the scale of a mineral crystal or contact between two crystals at low temperatures. Indeed, chemical solutions must be heterogeneous even at a scale of individual crystals because of incongruent dissolution of crystals (Lin and Clemency, 1981) and very sluggish rates of homogenization of chemical systems at low temperatures. Even small differences in the activities of alkalis and H^+ can result in the formation of kaolinite in place of smectite (Garrels and Christ, 1965; Hemley and Jones, 1964; Helgeson *et al.*, 1969). If the activity ratio of H^+/K^+ is relatively high, the formation of kaolinite is favored. The single observation of I/S as an apparent intermediate alteration product between muscovite and kaolinite may therefore simply have been due to local differences in solution chemistry.

Alternatively, the occurrence of smectite, illite, or I/S as an intermediate alteration product is reasonable from the point of view of the Ostwald step rule. Such 2:1 phases have structures very similar to that of muscovite. If structural differences are the principal consideration for the activation of alteration, the natural path for continuous change would therefore be in the sequence muscovite → illite → smectite → kaolinite. Thermodynamic conditions for which kaolinite is the stable phase could therefore give rise to illite or smectite as intermediate products. The presence of only a single observation of this sequence may simply be due to relatively rapid propogation of the alteration front along layers, once it was initiated, and/or to local differences in fluid chemistry.

ACKNOWLEDGMENTS

We are grateful to D. Craw and D. S. Coombs at the University of Otago, New Zealand, for helping D. R. Peacor collect samples and for sending us other samples. We also thank Jung Ho Ahn for helping with sample preparation. This work was supported by NSF grants EAR-86-04170 and EAR-88-17080 to D. R. Peacor.

REFERENCES

Ahn, J. H. and Peacor, D. R. (1986) Transmission and analytical electron microscopy of the smectite-to-illite transition: *Clays & Clay Minerals* **34,** 165–179.

Ahn, J. H. and Peacor, D. R. (1987) Kaolinitization of biotite: TEM data and implications for an alteration mechanism: *Amer. Mineral.* **72,** 353–356.

Bailey, S. W. (1980) Summary of recommendations of AIPEA Nomenclature Committee: *Clay Minerals* **28,** 73–78.

Bailey, S. W., Brindley, G. W., Johns, W. D., Martin, R. T., and Ross, M. (1971) Summary of national and international recommendations on clay mineral nomenclature 1969–70 CMS Nomenclature Committee: *Clays & Clay Minerals* **19,** 129–132.

Banfield, J. F. and Eggleton, R. A. (1988) Transmission electron microscope study of biotite weathering: *Clays & Clay Minerals* **36,** 47–60.

Banfield, J. F. and Eggleton, R. A. (1990) Analytical transmission electron microscope studies of plagioclase, muscovite, and K-feldspar weathering: *Clays & Clay Minerals* **38,** 77–89.

Beaufort, D. and Meunier, A. (1983) Petrographic characterization of an argillic hydrothermal alteration containing illite, K-rectorite, K-beidellite, kaolinite and carbonates in a cupromolybdenic porphyry at Sibert (Rhone, France): *Bull. Mineral.* **106,** 535–551.

Bell, T. E. (1986) Microstructure in mixed-layer illite/smectite and its relationship to the reaction of smectite to illite: *Clays & Clay Minerals* **34,** 146–154.

Brindley, G. W. and Pedro, G. (1972) Report of the AIPEA Nomenclature Committee: *AIPEA Newsletter No. 7,* 8–13.

Craw, D., Coombs, D. S., and Kawachi, Y. (1982) Interlayered biotite-kaolin and other altered biotites, and their relevance to the biotite isograd in eastern Otago, New Zealand: *Mineral. Mag.* **45,** 79–85.

Dudoignon, P., Beaufort, D., and Meunier, A. (1988) Hydrothermal and supergene alterations in the granitic cupola of Montebras, Creuse, France: *Clays & Clay Minerals* **36,** 505–520.

Eggleton, R. A. (1984) Formation of iddingsite rims on olivine: a transmission electron microscope study: *Clays & Clay Minerals* **32,** 1–11.

Eggleton, R. A. and Buseck, P. R. (1980) High-resolution electron microscopy of feldspar weathering: *Clays & Clay Minerals* **28,** 173–178.

Eggleton, R. A. and Boland, J. N. (1982) Weathering of enstatite to talc through a sequence of transitional phases: *Clays & Clay Minerals* **30,** 11–20.

Garrels, R. M. and Christ, C. L. (1965) *Solutions, Minerals and Equilibria,* Harper and Row, New York, 450 pp.

Guthrie, G. D., Jr. and Veblen, D. R. (1989) High-resolution electron microscopy of mixed-layer illite/smectite: Computer simulations: *Clays & Clay Minerals* **37,** 1–11.

Helgeson, H. C., Brown, T. H., and Leeper, R. H. (1969) *Handbook of Theoretical Activity Diagrams Depicting Chemical Equilibria in Geologic Systems Involving an Aqueous Phase at One Atm and 0° to 300°C,* Freeman, Cooper, San Francisco, 253 pp.

Hemley, J. J. and Jones, W. R. (1964) Chemical aspects of hydrothermal alteration with emphasis on hydrogen metasomatism: *Econ. Geol.* **59,** 538–569.

Hutton, C. O. and Turner, F. J. (1936) Metamorphic zones

in northwest Otago: *Royal Soc. New Zealand Trans.* **65,** 405–406.

Jiang, W.-T., Peacor, D. R., Merriman, R. J., and Roberts, B. (1990) Transmision and analytical electron microscopic study of mixed-layer illite/smectite formed as an apparent replacement product of diagenetic illite: *Clays & Clay Minerals* **38,** 449–468.

Klimentidis, R. E. and Mackinnon, D. R. (1986) High-resolution imaging of ordered mixed-layer clays: *Clays & Clay Minerals* **34,** 155–164.

Lee, S. Y., Jackson, M. L., and Brown, J. L. (1975) Micaceous occlusions in kaolinite observed by ultramicrotomy and high resolution electron microscopy: *Clays & Clay Minerals* **23,** 125–129.

Lin, F.-C. and Clemency, C. V. (1981) The kinetics of dissolution of muscovites at 25°C and 1 atm CO_2 partial pressure: *Geochim. Cosmochim. Acta* **45,** 571–576.

Lorimer, G. W. and Cliff, G. (1976) Analytical electron microscopy of minerals: in *Electron Microscopy in Mineralogy,* H.-R. Wenk, ed., Springer-Verlag, New York, 506–519.

Meunier, A. and Velde, B. (1979) Weathering mineral facies in altered granites: The importance of local small-scale equilibria: *Mineral. Mag.* **43,** 261–268.

Murray, H. H. (1988) Kaolin minerals: Their genesis and occurrences: in *Hydrous Phyllosilicates (Exclusive of Micas),* S. W. Bailey, ed., *Reviews in Mineralogy* **19,** Mineralogical Society of America, Washington, D.C., 67–89.

Nagasawa, K. (1978) Kaolin minerals: in *Clays & Clay Minerals of Japan,* T. Sudo and S. Shimoda, eds., Elsevier, New York, 189–219.

Olives, J. O. and Amouric, M. (1984) Biotite chloritization by interlayer brucitization as seen by HRTEM: *Amer. Mineral.* **69,** 869–871.

Sharp, T. G., Otten, M. T., and Buseck, P. R. (1990) Serpentinization of phlogopite phenocrysts from a micaceous kimberlite: *Contrib. Mineral. Petrol.* **104,** 530–539.

Stoch, L. and Sikora, W. (1976) Transformation of micas in the process of kaolinitization of granites and gneisses: *Clays & Clay Minerals* **24,** 156–162.

Turner, F. J. (1935) Metamorphism of the Te Anau Series in the region north-west of Lake Wakatipu: *Royal Soc. New Zealand Trans.* **65,** 329–349.

Veblen, D. R. and Ferry, J. M. (1983) A TEM study of the biotite-chlorite reaction and comparison with petrologic observations: *Amer. Mineral.* **68,** 1160–1168.

Veblen, D. R., Guthrie, G. D., Jr., Livi, K. J. T., and Reynolds, R. C., Jr. (1990) High-resolution transmission electron microscopy and electron diffraction of mixed-layer illite/smectite: Experimental results: *Clays & Clay Minerals* **38,** 1–13.

Yau, Y.-C., Anovitz, L. M., Essene, E. J., and Peacor, D. R. (1984) Phlogopite-chlorite reaction mechanisms and physical conditions during retrograde reactions in the Marble Formation, Franklin, New Jersey: *Contrib. Mineral. Petrol.* **88,** 299–306.

Yau, Y.-C., Peacor, D. R., and McDowell, S. D. (1987) Smectite-to-illite reactions in Salton Sea shales: A transmission and analytical electron microscopy study: *J. Sediment. Petrol.* **57,** 335–342.

(Received 13 January 1990; accepted 9 September 1990; Ms. 1976)